Available online at www.pelagiaresearchlibrary.com

Pelagia Research Library

Advances in Applied Science Research, 2011, 2 (5): 173-184

ISSN: 0976-8610
CODEN (USA): AASRFC

Structural, Optical and Electrical Properties of Chemically Grown $Zn_{1-X}Hg_XSe$ (x= 0-1) Semiconductor Thin Films

B. R. Arbad[a], U. R. Dappadwad[a] and V. M. Bhuse[b*]

[a]Department of Chemistry, Dr. B. A. M. University, Aurangabad, M. S, India
[b]Department of Chemistry, Thin Film Research Laboratory, Rajaram College, Vidyanagar, Kolhapur, Maharashtra State, India

---

ABSTRACT

The Cadmium mercury chalcogenides (CMC's) have been considered as an important material for use in optoelectronic devices. These compounds, however, possess limitations on the ultimate efficiency and stability of devices due to weak nature of Hg-Se bond. The major consequences faced are lattice instability, poor mechanical, optical and electrical properties. The replacement of 'cadmium' by 'zinc' has been shown to enhance overall stability and better optoelectronic properties. In view of this, we report, a simple, aqueous chemical route to grow a full range of $Zn_{1-X}Hg_XSe$*(x= 0-1) alloy semiconductor system on glass substrate at room temperature with special emphasis on their structural, optical and electrical properties. The XRD study revealed the polycrystalline nature for all compositions in a single cubic phase. The film were uniform, adherent, with color varying from faint yellow(for ZnSe) to dark red(for HgSe) as mercury content was increased. The lattice constant registers a small deviation in Vegard's law for compositions (x)* ≥ 0.6*; while the band gaps were found to bow above the linearity function. The electrical conductivity and activation energies were found to a function of composition, x. Chemical deposition system is useful in depositing ZMS film of desired properties by careful selection of compositional parameter (x).*

Keywords: Chemical deposition, II-VI semiconductors, Thin films, X ray diffraction, Electron microscopy.

INTRODUCTION

The pseudo-binary compounds of IIB group cations and VIA group anion of the periodic table attracts a great deal of attention due to their potential optoelectronic usage, especially in IR detection and solar cell technology [1-4]. These alloy offer composition based modulation of their semiconductor properties viz. electrical, band gap, lattice constant etc. Among these, Zinc mercury selenide (ZMS), offers a special interest over cadmium based chalcogenide systems due to (i) presence of excess electrical carriers [5], (ii) greater stability since HgSe bond is shorter and stronger than HgTe (iii) additional lattice stability since presence of Zinc is less destabilizing than Cadmium [6], (iv) smooth modulation of properties as Zn dissolves completely in HgSe [7], (v) good absorption of photon of light (ZMS limiting value ~2.8 eV while for CMT limiting value ~2.5 eV) [8], (vi) higher micro-hardness of HgSe based alloy [9] (vii) stability of optical properties [10] (viii) higher crystallinity [11] and (ix) lesser compositional variations and surface sensitivity [12].

The characteristics thus illustrated make ZMS an interesting candidate in applications such as solar cell and electromagnetic radiation detection. In spite of its potential advantages over cadmium mercury chalcogenides (CMC) alloy, the work reported on ZMS thin film is quite limited. So far, few reports are available on ZMS [3,8,11,13-16]. The literature survey indicated that no attempt have been made to develop the ZMS using a cost effective chemical bath deposition technique. In our previous paper [2], we reported, the synthesis of $Zn_{0.5}Hg_{0.5}Se$ using chemical bath and discussed the characteristic properties.

In this paper we report a low temperature chemical bath methodology to prepare stiochiometric, polycrystalline $Zn_{1-x}Hg_{1-x}Se$ system in whole range of compositions. So far, this method have been used successfully for the deposition of stiochiometric CdHgSe [17], CdHgTe [18] ,CdPbSe [19] materials in thin film form. Now a day, this method has shown to be versatile technique to deposit high quality semiconductor layers belonging to other group of periodic table [20, 21], even in nanocrystalline form [22].

MATERIALS AND METHODS

All the chemicals used were of Analytical Reagent grade (E-Merk). Doubly distilled water was used to prepare solutions. All the solutions were stored in a stoppered borosilicate glass. The micro glass slides were used as substrates to deposit material in thin film form.

2.1 Substrate Cleaning

The cleaning of micro glass slides was done by thorough and successive washings with chromic acid and deionized water.

2.2 Preparation of Anionic Precursor

A metastable anionic precursor, sodium selenosulphate was prepared by dissolving 5 gm (excess) finely powered grey selenium metal in 200 ml, 0.25 M solution of Sodium sulphite by refluxing at 90^0C temperature for 9 hours. The solution is stored in stoppard glass bottle to avoid contact with atmospheric air (as it slowly oxidizes to metallic selenium).

2.2. Preparation of Cationic Precursor

A cationic precursor was prepared by mixing volume stiochiometric mixtures of mercuric nitrate (0.25M), zinc nitrate (0.25M) corresponding to composition parameters (x) and ammonia (25% v/v, 40 ml) (as complexing agent) with vigorous stirring. For example, to prepare $Zn_{0.4}Hg_{0.6}Se$ film, we used 4 ml of 0.25 M Zinc nitrate and 6 ml of 0.25 M mercury nitrate. The nitrate salts are preferred as Hg form soluble complex in presence of nitrates only.

2.3. Preparation of Thin Films

The method used to prepare film is as follows; 10 ml of cationic precursor solution was diluted using previously cooled, doubly distilled water to 150 ml (taken in a 250 ml capacity beaker). This beaker was transferred to a bath of 278 K temperature. To this, 10 ml of 0.25 M sodium selenosulphate solution was added slowly. Previously cleaned glass slides (substrates), mounted on specially designed substrates were rotated in solution at a speed of 45±2 rpm using an electric motor. The temperature of the bath was then allowed to increase up to 300 K slowly. After about three hours, the slides coated with films were removed, washed with deionized water, dried naturally and kept in dark desiccator over anhydrous $CaCl_2$.

2.4 Film Characterization

X-ray diffraction pattern of films were recorded (Philips pw-1710) in 2θ range from 10 to 80^0 with Cu $K\alpha_1$ line (1.54056Å).The electrical resistance measurements were carried on Zintek-502BC Milliohmmeter in 300-500K temperature range. Hitachi-330 (Japan) double beam spectrophotometer was used to record optical absorption spectra in 350-1100 nm wavelength range at room temperature. A 250 MK-III stereoscan (U.S.A.) Scanning Electron Microscope (SEM) was used to observe the surface morphology of the film material. The quantities of Zn and Hg were determined by using AAS while selenium was estimated by following a standard gravimetric method [23].

RESULTS AND DISCUSSION

3.1 Growth Kinetics & Physical Properties

The decomposition of ammonia complexes of Zn^{2+}, Hg^{2+} and Sodium selenosulphate were made possible by a slow increase in the temperature of bath. The decomposition reactions generate bare ions that may combine initially on the surface of the substrate to give nucleation centers, these centers grow further by absorbing more and more ions to give a film (and also precipitate in solution).

The following are proposed reactions sequence for film formation;

$Zn^{+2} + 4NH_3 \leftrightarrow Zn(NH_3)_4]^{2+}$ (Complex formation) (1)

$Hg^{+2} + 4NH_3 \leftrightarrow Hg(NH_3)_4]^{2+}$ (Complex formation, in nitrate medium only) (2)

$Na_2SO_3 + Se \rightarrow Na_2SeSO_3$ (metastable sodiumselenosulphide formation) (3)

$Zn(NH_3)_4]^{2+} \leftrightarrow Zn^{+2} + 4NH_3$ (Complex dissociation) (4)

$Hg(NH_3)_4]^{2+} \leftrightarrow Hg^{+2} + 4NH_3$(Complex dissociation) (5)

$Na_2SeSO_3 + OH- \rightarrow Na_2SO_4 + HSe^-$

$HSe^- + OH^- \rightarrow H_2O + Se^{-2}$ (6)
(metastable sodiumselenosulphide decomposition in alkaline medium)

$(1-x)Zn^{+2} + xHg^{+2} + Se^{-2} \rightarrow Zn_{1-X}Hg_XSe$ (ionic combination) (7)

The overall reaction can be written as;

$(1-x)[Zn(NH_3)_4] + x\,[Hg(NH_3)_4] + Se^{-2} \rightarrow Zn_{1-X}Hg_XSe + 8NH_3$ (8)

The growth process depends upon the solubility constants of HgSe and ZnSe and the temperature of the bath. The HgSe is having low solubility product than ZnSe, so it is assumed that HgSe should be forming initial nucleation centers which grow further by accumulation of Zn and Hg ions. A chemical bath method involves combination of oppositely charged ‘cations’ with ‘anions’, and as the combination being systematic and stiochiometric, it always result in homogeneous compound / alloy even at low temperature [2,17-18]. All the cations are divalent, belong to the same group therefore, co-precipitation process makes no discrimination between them. It is to be noted that other method involves combinations of uncharged ‘atoms’ or ‘molecules’, which ultimately results in random gathering of atoms/ions giving some sort of non-homogeneity and hence non-stiochiometry.

In chemical bath deposition, a slow and uniform churning of the bath solution is quite essential to keep ‘homogeneity’ of ions in the solution and thus in the film.

3.2 Structural Investigations

The zinc selenide and mercury selenide in bulk exist in both wurtzite (hexagonal) and Sphalerite (cubic, zincblende) structures, however the alloy of both, is reported to exist in zinc blend structures only [7]. The x ray pattern of as deposited ZnSe and HgSe films along with ASTM pattern (in line form, from JCPDS Card No 75-1554 & 37-1463 respectively) is displayed in figure 1, while figure 2 show peak patterns of five representative films with compositions 0.1, 0.3, 0.5. 0.7 and 0.9. The comparisons of observed peak pattern with those given in ASTM data suggest presence of a single cubic structure for all the films. The XRD pattern of HgSe exhibits a sharp peak pattern while that of ZnSe exhibit growth of prominent peaks over some amorphous background.

All the film show characteristic XRD line pattern of FCC structure, where a pattern of a single peak, followed by two adjacently spaced peaks is repeated, therefore, all peaks were recognized as reflections originating from 111, 200, 220, 311, 222, 331 planes of zinc blend lattice. The XRD pattern of ZMS (x=0.1–0.9) showed systematic shifting of diffraction line angle toward lower 2θ positions with progressive inclusion of Hg. The intensity of peaks, especially 111 peak, was observed to increase continuously with increase in Hg content suggesting that the crystallinity is getting improved progressively with predominant growth along 111 direction. The lattice parameters have been calculated for all the compositions and are listed in table 1. The lattice constant of ZMS alloy registers a systematic increase in magnitude with increase in Hg concentration. This is usual as bigger sized Hg ion (size Hg -0.148 nm) is being incorporated in the lattice in place of Zn ions (size of Zn - 0.131 nm) forming solid solutions. The absence of peaks corresponding to pure cubic / hexagonal ZnSe, HgSe or alloy in hexagonal phase support this inference.

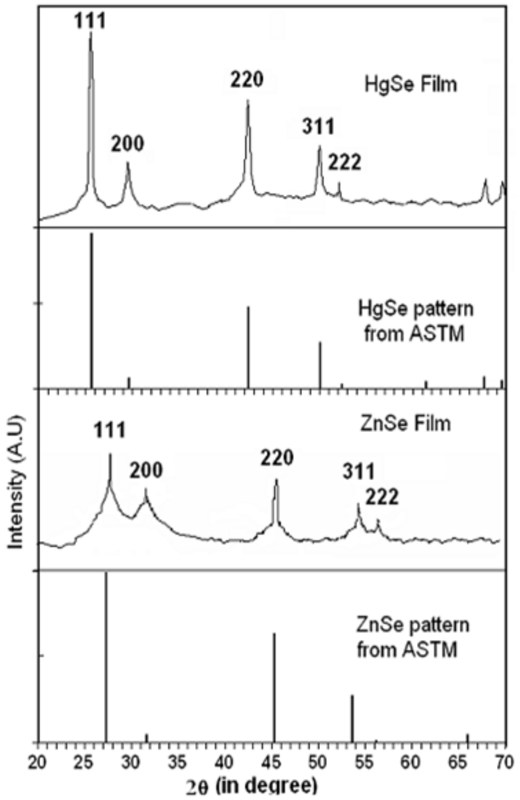

Fig. 1 X-ray diffraction pattern of pure HgSe and pure ZnSe along with their ASTM data (shown in line form)

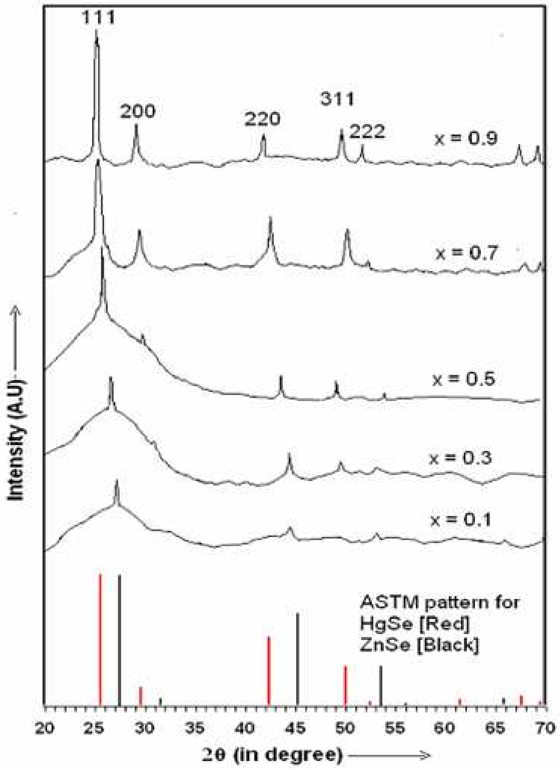

Fig.2 X-ray diffraction pattern of as deposited $Zn_{1-x}Hg_xSe$ thin films with x= 0.1, 0.3, 0.5, 0.7, 0.9 along with the ASTM pattern in line form.

The dependence of lattice constant on composition parameter (x) (Figure 3) shows a linear variation for compositions up to x = 0.5, thereafter quasi-linear behavior, thus registering a little deviation in Vegard's law for higher x.

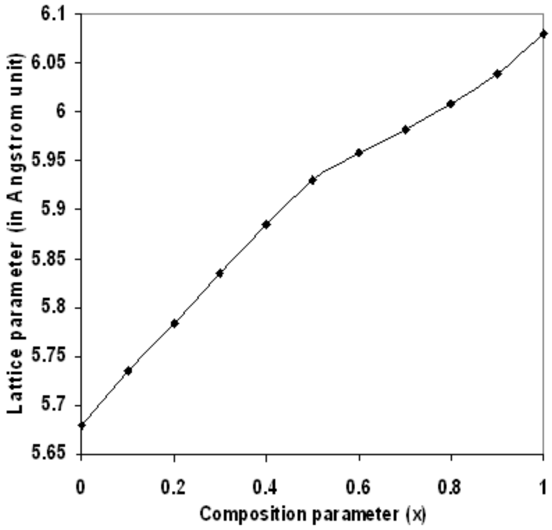

Fig.3 A variation of lattice constants with composition parameter (x) of films.

The initial linear increase can be attributed to filling of tetrahedral holes (i.e. Zn sites) by Hg ions of higher size in the lattice of ZnSe, however, beyond x = 0.5, the saturation might be occurring so that there is a little room to expand the cell causing quasi-linear variation. This effect may be brought about by higher nuclear power of Hg ion in the Zinc blende lattice. The lattice of ZMS is isomorphus to ZnSe and HgSe, with Zn/Hg occupying 4c lattice sites (a/4 places) randomly. The lattice has a typical structure with all Se ions situated in the perimeter of cube that largely determines the cell size of the alloy. The zinc bende lattice is known to have a lowest packing fraction (34%). This makes a sort of compensation for nuclear power at higher concentration of Hg (i.e. x >0.5) leading to observed result. The number of atoms per cell was calculated from x-ray density was found to be eight atoms or four molecules per cell.

3.3 Morphological and Compositional Studies

The surface morphology of few representative $Zn_{1-x}Hg_xSe$ alloy thin films is displayed in Figure 4. In general, the films are homogenous with grains well covered on the glass substrate, without any cracks or pinholes. The grains were found to be grown over a smooth, homogenous background supporting the typical deposition involving one step growth by multiple nucleations. The ZnSe showed somewhat amorphous behavior. All other film exhibit smooth, compact surface due to uniform distribution of spherical shaped grains of almost same size. We do not observe any agglomeration or fusion of smaller crystallite (except for films with x = 0.1) as usually observed in deposits obtained by electrodeposition method [8]. The grain size was observed to increase with addition of mercury in ZnSe. The color of alloy film was found to vary from light yellow to dark red as mercury content is increased.

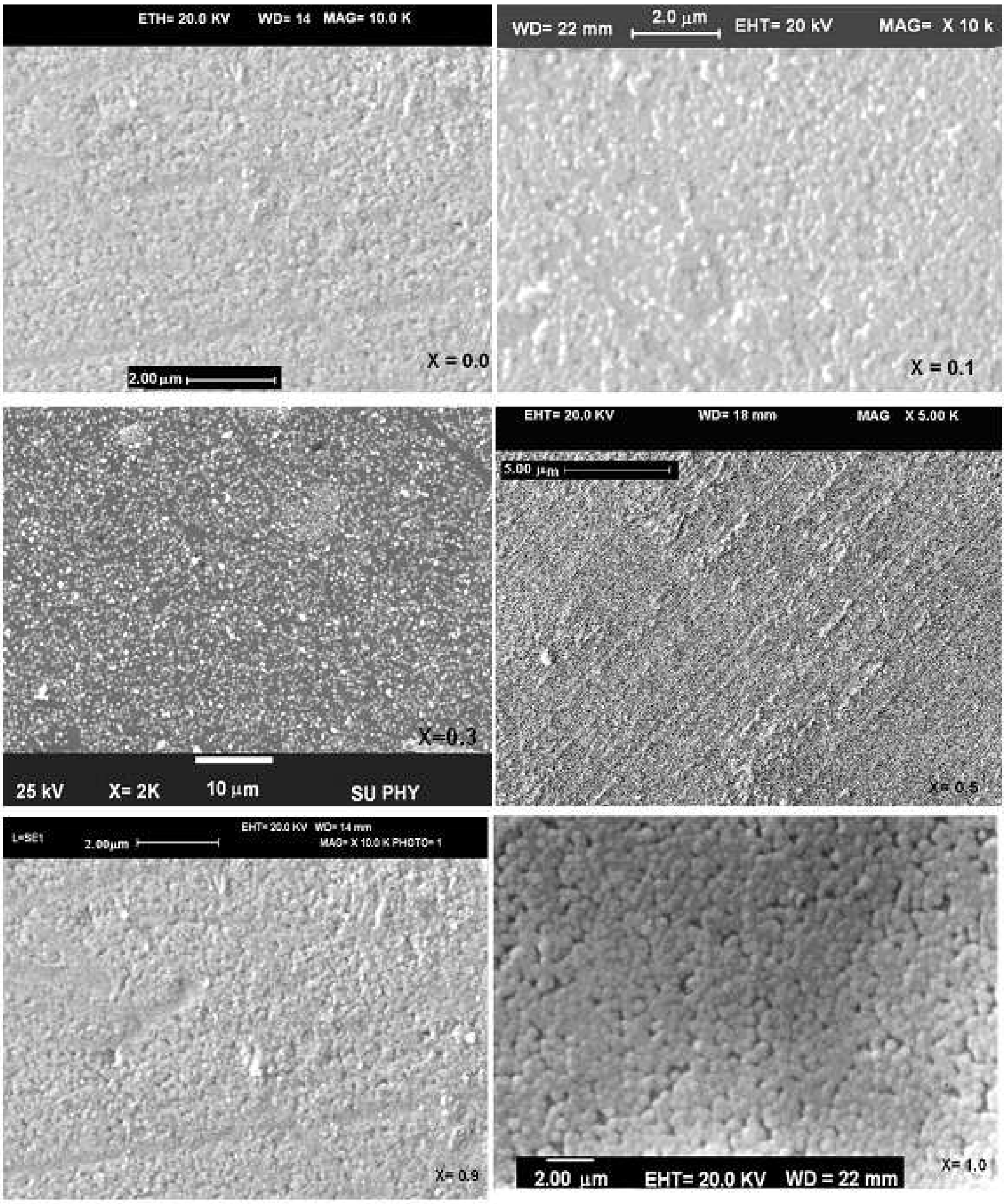

Fig.4 Surface morphology of $Zn_{1-x}Hg_xSe$ alloy thin films with compositions; x= 0.0, 0.1, 0.3, 0.5, 0.9 & 1.0

Atomic absorption spectroscopy was used to determine the quantity of zinc and mercury content in the film samples. A known weight of film material was dissolved in minimum quantity of concentrated HNO_3 acid so that Zn and Hg goes into solution as soluble salts and a red precipitates of selenium is obtained, which is measured gravimetrically [23]. After removing Selenium, the remaining solution was diluted appropriately to measure quantities of Zn and Hg using AAS. The observed composition of zinc, mercury and selenium in the films are reported in the table 1. The data obtained imply that the ratio of content of film match well with those taken in bath within 5% error limit.

3.4 Optical Band Gap Studies

The optical absorption spectra were analyzed to determine various parameters like absorption coefficient, nature of transitions involved and magnitude of band gaps. The optical absorption coefficient computed for all the composition was found to be high; of the order of 10^4 cm^{-1} (data not shown) and that the magnitude increases with concentration of mercury. The general observation regarding the absorption edge is that it shifts toward the low energy region of the uv-vis spectrum (red shift) with addition of Hg and that no multiple edges were observed. This observation, coupled with the XRD and compositional analysis strengthen the formation of alloy films over the whole range studied. The absorption spectra for $Zn_{1-X}Hg_XSe$ shows sharpening of absorption edge with the inclusion of Hg ions into the lattice of ZnSe.

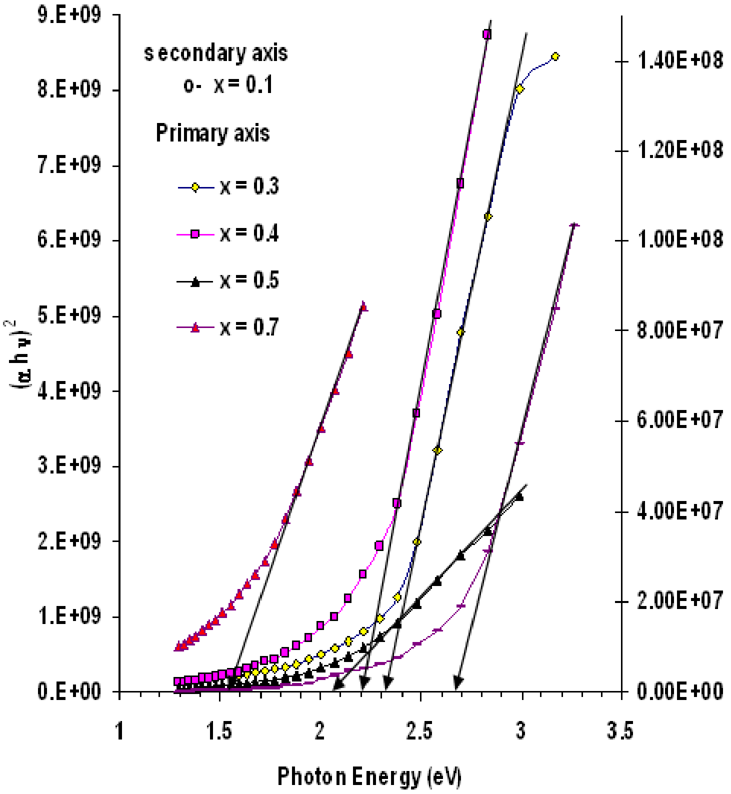

Fig.5 $(\alpha h\nu)^2$ Vs.hν plots for $Zn_{1-x}Hg_xSe$ alloy thin films with x = 0.1, 0.3, 0.4, 0.5, 0.7.

The absorption data in the vicinity of an absorption edge was analyzed using a well known equation [24];

$$\alpha h\nu = A (h\nu - Eg)^r \qquad (9)$$

Where ‘r’ depend on the kind of transitions involved and takes value 1/2, 2, 3/2, 3 for direct allowed, direct forbidden, indirect allowed, indirect forbidden transitions respectively. A is a constant depending upon the temperature, α is an absorption coefficient and hν is the phonon energy, etc. For valid r, a plot of $(\alpha h\nu)^{1/r}$ vs. hν should exhibit linear dependence so that extrapolation of the linear portion of curve at energy axis gives the respective optical band gap. Accordingly we observed a best fit for all the film samples at r = ½, corresponding to presence of a single, direct allowed type band gap. Figure 5 shows $(\alpha h\nu)^2$ Vs. hν plots for few representative samples (with x=0.1, 0.3, 0.4, 0.5 & 0.7). The values of band gap thus obtained are listed in table 1.

The band gaps for ZMS were found to fall within 0.81 to 2.71 eV range, the extremes values corresponds to band gap of HgSe and ZnSe respectively. The magnitude of band gap of ZnSe was found to match with those reported in the literature [25]. In case of HgSe, there exists a large disparity in its band gap. Although the bulk HgSe is regarded as semimetal due to inverted type structure, there are several reports available on thin HgSe films so that it can be considered as semiconductor material having bandgap of magnitude around 0.81 eV [26-28]. The band gap of ZMS varies systematically within those of two extremes; however this dependence is not perfect linear function of composition parameter, thus registering a little deviation. There is, however, no data available on the band gaps of full range of ZnHgSe alloy system to compare with. Kashyap et al. [15] studied the optical properties of flash evaporated thin polycrystalline $Zn_{1-x}Hg_xSe$ films over the entire composition range and reported a strong nonlinear dependence of band gaps on x with a bowing following a parabolic dependence obeying relation;

$$Eg(x) = -0.07 + 0.49x + 2.18x^2 \qquad (10)$$

While Gavaleshko et al [16] reported nonlinear variation of ZMS for x between 0- 0.15.

These nonlinear variations observed in ref. [15] & [16] are probably associated with inhomogeneity of the deposits obtained by other than CBD methods. As far as our results are concerned, we do not observe any non linear variation. A small positive bowing was however observed that can be ascribed due to local lattice disorder. Similar kind variations have been observed in cases of chemically deposited CdHgSe [17], CdHgTe [18] and CdPbSe [19] thin films. It is to be noted here that the method of chemical deposition involves the building of crystals by arranging the charged particles (cations & anions) systematically, while other methods (like electrodeposition, vapour deposition methods etc) utilizes atoms for building the crystals. Thus chemical bath method arranges ions more orderly than other methods leading to homogenous deposits.

The linear variation of band gap, within two extremes is an indication of the fact that Zn is being displaced regularly and homogeneously by Hg in ZnSe lattice giving alloy films.

3.5 Electrical Properties

The variations of dark ‘dc’ electrical conductivity of as deposited films on non-conducting glass slide with temperature were studied using a conventional two probe method, in the temperature range 300–525K. At room temperature, the specific conductance of ZnSe was found to be lower (by two orders of magnitude) than those reported in [29] while for HgSe, it was found to match well with the published data [26-28]. The dark specific conductance of the ZMT films at room temperature were found to be between 2.0 $x10^{-2}$ to $3.1x10^{-6}$ $(\Omega.cm)^{-1}$ (table 1). The values of specific conductance at 300 K for films with lower x are low due to low crystallinity of the alloy. The Arrhenius plot for ZnSe and $Zn_{1-x}Hg_xSe$ films with $x \geq 0.5$, showed linear dependence of conductivity on temperature; this is an indication of the presence of only one type i.e. intrinsic type of conduction mechanism. While for $x < 0.4$, two distinct linear regions corresponding to the low-temperature extrinsic (impurity) and high temperature intrinsic regions were observed. The low temperature region corresponds to extrinsic (variable range hopping) and high temperature corresponds to intrinsic conductivity as usually obtained in alloy type of semiconductor (Figure 6). The activation energies were calculated from the slope of Arrhenius plot and are included in table 1. Both the activation energies were found to decrease almost linearly with increase in mercury content, the fact can be correlated to decrease on gap between valence and conduction band of alloy.

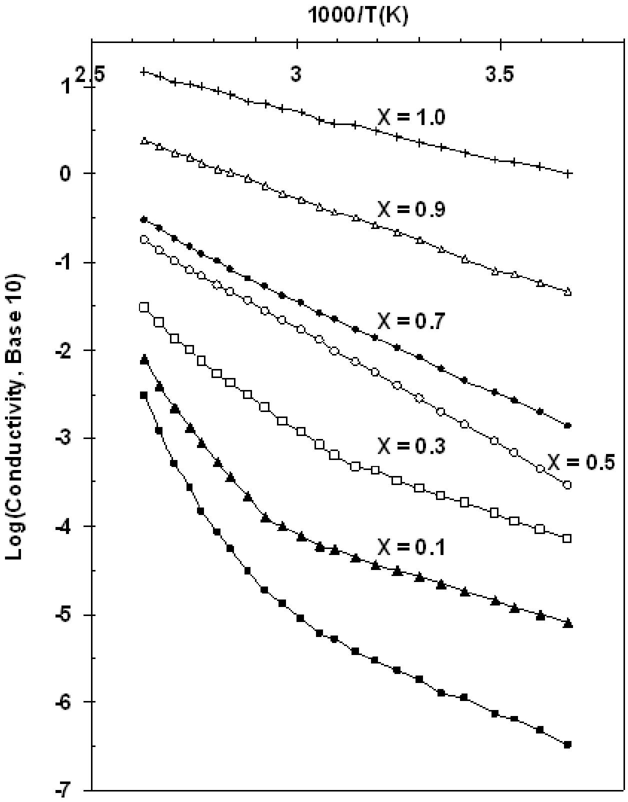

Fig.6 Arrhenius plot for films with x = 0.1, 0.3, 0.5, 0.7, 0.9, 1.0.

Table 1: Lattice parameters, Bandgaps, Compositions, Specific conductance and activation energy data of ZMT film materials

Film composition	**Cell size in Å**	**Bandgap in eV**	**Zn:Hg ratio**		**Activation energy in eV**	
			Observed	**Taken**	**Low T**	**High T**
ZnSe	5.68	2.81	-	-	0.025	0.63
$Zn_{0.9}Hg_{0.1}Se$	5.735	2.68	8.73	9.00	0.023	0.58
$Zn_{0.8}Hg_{0.2}Se$	5.784	2.56	3.76	4.00	0.019	0.54
$Zn_{0.7}Hg_{0.3}Se$	5.835	2.32	2.31	2.34	0.016	0.50
$Zn_{0.6}Hg_{0.4}Se$	5.884	2.21	1.48	1.50	0.013	0.46
$Zn_{0.5}Hg_{0.5}Se$	5.93	2.08	0.98	1.00	-	0.43
$Zn_{0.4}Hg_{0.6}Se$	5.958	1.81	0.66	0.67	-	0.38
$Zn_{0.3}Hg_{0.7}Se$	5.982	1.53	0.43	0.43	-	0.31
$Zn_{0.2}Hg_{0.8}Se$	6.007	1.31	0.26	0.25	-	0.23
$Zn_{0.1}Hg_{0.9}Se$	6.038	1.07	0.11	0.11	-	0.15
HgSe	6.08	0.81	-	-	-	0.08

CONCLUSION

A ternary ZMS alloy material can be synthesized in whole range easily by employing chemical bath method. The method follows ion by ion combinations to yield homogeneous and stiochiometric alloy in a single cubic phase. The band gaps of ZMS vary almost linearly with lowering of Hg content, while electrical conductivities ranges from 10^{-2} to 10^{-6} (ohm cm)$^{-1}$. Using CBD, it is possible to deposit ZMS film of desired properties by careful selection of compositional parameter (x).

Acknowledgements

One of the authors (VMB) is thankful to the Director, Higher Education, Maharashtra State and Principal, Rajaram College, Kolhapur, for their constant support to carry out this research work.

REFERENCES

[1] V.M. Bhuse, P.P. Hankare, S. Sonandkar, *Mat. Chem. Phys.*, **2007**, 101, 303.

[2] U.R. Dappadwad, M.K. Lande, S.G. Chonde, B.R. Arbad, P.P. Hankare, V.M. Bhuse, *Materials Chemistry and Physics*, **2008**, 112, 941.

[3] T. Mahalingam, A. Kathalingam, S. Velumani, Soonil Lee, Kyeung Seek Lew and Yong Deak Kim, *Semicond. Sci. Technol*., **2005**, 20, 749.

[4] J. M. Gaines, R. R. Drenten, K. W. Haberern, T. Marshell, P. Mensz and J. Petruzzello, *Appl. Phys. Lett.*, **1993**, 62, 2462.

[5] S. D. Cobb, F.R. Szofran, K.S. Jones, S. L. Lehoczky, *J. Elect. Mat*., **1999**, 28, 732.

[6] A. Sher, A. B. Chen, W.E. Spicer and C. K. Shih, *J. Vac. Sci. technol*., **1983**, A3, 105.

[7] K. Kumazaki, I. Vina, C. Umbach and M. Cardona, *Solid State Communications*, **1988**, 68, 591.

[8] Hosun Moon, A. Kathalingam, Thaiyan Mahalingam, J. P. Chu, Yong Deak Kim, *J. Material Science: Materials in Electronics*, **2007**, 18, 1013.

[9] R. N. Andrews, S. D. Walck, M. W. Price, F. R. Szofran and S. L. Lehoczky, *J. Crystal Growth*, **1990**, 99, 717.

[10] S.D. Cobb, R.N. Andrews, F.R. Szofran and S.L. Lehoczky, *J. Cryst. Growth*, **1991**, 110, 415.

[11] C. Natrajan, M. Sharon, C. Levy Clement, M. Neumann Spallart, *Thin Solid Films*, **1995**, 257, 46-53.

[12] W. E. Tennant, C. A. Cockrum, J. B. Gilpin, M. A. Kinch, M. B. Reine, R. P. Ruth, *J. Vac. Sci. & Technol.*, **1992**, B 10, 1359.

[13] S. Einfeldt, U. Lunz, H. Heinke, C.R. Becker, C. Landwehr, *J. Crystal Growth*, **1995**, 146, 427.

[14] T. Behr, S. Einfeldt, D. Hommel, C. R. Becker, G. Landwehr, H. Cerva, *J. Crystal Growth*, **1996**, 159, 1123.

[15] P. Kashyap, M. Jain, H. K. Sehgal, *Infrared Physics*, **1990**, 30, 343.

[16] N.P. Gaveleshko, P.N. Gorley, V.V. Khomyak, V.A. Shenderovskii, *Phys. Stat. Sol*. (b), **1980**, 98, 463.

[17] P.P. Hankare, P.A. Chate, S.D. Delekar, V.M. Bhuse, M.R. Asabe, B.V. Jadhav, K.M. Garardkar, *J. Crystal Growth*, **2006**, 291, 40.

[18] B.R. Arbad, S.G. Chonde, P.P. Hankare, V.M. Bhuse, *Arch. Appl. Sci. Res*, **2011**, 3(2) , 422.

[19] P. P. Hankare, S. D. Delekar, P. A. Chate, S. D. Sabane, K. M. Garadkar and V. M. Bhuse, *Semicond. Sci. Technol.*, **2005**, 20, 257.
[20] A.J. Ragina, K.C. Preetha, K.V. Murali, K. Deepa, T.L. Ramadevi, *Adv. Appl. Sci. Res*, 2(3) (**2011**) 438-444.
[21] S. Srikanth, N. Suriyanarayanan, S. Prabhakar, V. Balsubramanian, D. Kathirvel, *Adv. Appl. Sci. Res*, 2(1) (**2011**) 95-104.
[22] Y.V. Marathe, V.S. Shrivastava,, *Adv. Appl. Sci. Res*, 2(3) (**2011**) 295-301.
[23] G.H Jeffery, J. Bassett, J. Mendham, R.C. Denney, Vogel's Text Book of Quantitative Chemical Analysis, Fifth Edition, Longman Scientific & Technical, UK, **1989**, pp-46.
[24] J. I. Pankove in: (Ed: Englewood Cliffs) Optical Processes in Semiconductors, (Prentice Hall, NJ, **1971**) 92.
[25] V.M. Gracia, M.T.S. Nair and P.K. Nair, *Semicond. Sci. Technol.*, **1999**, 14, 366.
[26] P.P. Hankare, V.M. Bhuse, K.M. Garadkar, A.D. Jadhav *Materials Chemistry and Physics*, **2001**, 71, 53.
[27] T. Mahalingam, A. Kathalingam, C. Sanjeeviraja, R. Chandramohan, J.P. Chu, Yong Deak Kim and S. Velumani, *Materials Characterization*, **2007**, 58(8-9), 735.
[28] S. Y. Girgis, A. M. Salem and M. S. Selim, *J. Phys. Condens. Matter*, **2007**, 19**,** 116.
[29] P. P. Hankare, P. A. Chate , D. J. Sathe, P. A. Chavan , V. M. Bhuse, *J Mater Sci: Mater Electron.*, **2009**, 20, 374–379.